

Thermodynamic Analysis of Supercell Rear-Flank Downdrafts from Project ANSWERS

MATTHEW L. GRZYCH, BRUCE D. LEE, AND CATHERINE A. FINLEY

WindLogics, Inc., Grand Rapids, Minnesota

(Manuscript received 5 January 2006, in final form 26 April 2006)

ABSTRACT

Data collected during Project Analysis of the Near-Surface Wind and Environment along the Rear-flank of Supercells (ANSWERS) provided an opportunity to test recently published associations between rear-flank downdraft (RFD) thermodynamic characteristics and supercell tornadic activity on a set of 10 events from the northern plains. On average, RFDs associated with tornadic supercells had surface equivalent potential temperature and virtual potential temperature values only slightly lower than storm inflow values. RFDs associated with nontornadic supercells had mean group equivalent potential temperature and virtual potential temperature values that were colder relative to storm inflow values than their respective tornadic counterparts. Additionally, the analysis revealed that RFDs associated with tornadic supercells had higher CAPE and lower convective inhibition than the RFDs of nontornadic supercells, on average. The results of this study provide further support for the general concept that a thermodynamic delineation generally exists between the RFDs of tornadic and nontornadic supercells.

1. Introduction

The association between supercell thunderstorm rear-flank downdrafts (RFDs) and tornadoes has long been recognized (Markowski 2002a). More recent research has focused on direct measurements within the RFD by utilizing a mobile mesonet (Straka et al. 1996). The analysis of Markowski et al. (2002, hereafter MSR2002) and Markowski (2002b, hereafter M2002) revealed compelling evidence supporting the conclusion that tornado likelihood, intensity, and longevity were associated with the RFD thermodynamic characteristics. Specifically, the results of MSR2002 (and supported by M2002) showed that tornado likelihood, intensity, and longevity increase as the near-surface buoyancy, potential buoyancy [as indicated by the convective available potential energy (CAPE)], and equivalent potential temperature θ_e increase in the RFD and as the convective inhibition (CIN) in the RFD decreases.

This study was motivated by both the demonstrated importance of the RFD thermodynamic characteristics

(MSR2002; M2002) and the recognition that a nonexhaustive quantity of analyzed RFDs exist given the variety of potential scenarios leading to tornadogenesis. Further, because almost all of the MSR2002 RFD events were from the central or southern plains or adjacent high plains, the addition of analyzed RFD events from the northern plains (where all of the datasets analyzed in this paper were obtained) provides geographic diversity to the body of published RFD thermodynamic characterizations and an opportunity to compare the geographic consistency of the RFD thermodynamic signals. In total, the near-surface thermodynamic characteristics of 10 RFDs were analyzed (four tornadic and six nontornadic events). The following guiding hypothesis, adopted from the research of MSR2002, formed the basis of this study: RFDs characterized by small θ_e and θ_v perturbations (calculated from a comparison with storm inflow θ_e and θ_v values), the presence of CAPE, and small CIN are necessary for tornadogenesis.

The RFD datasets were collected during a field experiment called Project Analysis of the Near-Surface Wind and Environment along the Rear-flank of Supercells (ANSWERS) conducted during May and June of 2003. ANSWERS was designed to address a number of hypothesis-driven objectives that involve attributes of the RFD and RFD boundary (RFDB) environment pertaining to topics ranging from low-level mesocyclo-

Corresponding author address: Dr. Bruce D. Lee, WindLogics, Inc., Itasca Technology Exchange, 201 NW 4th Street, Grand Rapids, MN 55744.
E-mail: blee@windlogics.com

genesis and tornadogenesis (and maintenance) to gustnado occurrence. Consistent with these objectives, ANSWERS focused its meteorological sampling resources near the RFDB and within the RFD of tornadic and nontornadic supercell thunderstorms. The project domain included regions from the northern plains and upper Midwest through the southern plains; however, all of the quality RFD datasets were collected in South Dakota or northern Nebraska. ANSWERS typically utilized four mobile mesonet stations largely staffed by personnel associated with the University of Northern Colorado (UNC) and Texas Tech University with nowcast support from participants at UNC and the University of Illinois.

This paper is organized in the following way. Overviews of the mobile mesonet data and experiment methodology are presented in section 2. Thermodynamic characterization of the 10 RFD events and event type groupings are documented in section 3. In section 4, a summary of the RFD thermodynamic signals and a discussion of the results are presented.

2. Mobile mesonet data and methodology

The mobile mesonet (hereafter referred to as “mesonet”) measures temperature, pressure, humidity, and wind velocity. Time and position were recorded using a global positioning system. The type of instrumentation and mesonet station configuration were based on the design presented by Straka et al. (1996). The reader is referred to Straka et al. for an overview of the mesonet station configuration, instrumentation, and technical specifications. For some sensors, more recent or more accurate models of the instrumentation were used. Mesonet station data were recorded every 2 s.

Because of inaccuracies in the anemometry during significant vehicle accelerations, velocity data were removed in a manner similar to MSR2002 and M2002. The mesonet datasets were also quality controlled for spurious meteorological readings and vehicle headings. Biases were removed by way of intercomparisons between mesonet stations for approximate 20–30-min periods when the caravan was in relatively uniform meteorological conditions, usually en route to a target.

Derived thermodynamic variables were calculated in addition to the variables measured directly by the mesonet. As in MSR2002, θ_e was calculated using the formula derivation of Bolton (1980). In the calculation of the virtual potential temperature θ_v (Glickman 2000), no hydrometeors were assumed to be present. Because most ANSWERS data were collected on storms at a significant distance from the nearest Weather Surveillance Radar-1988 Doppler (WSR-88D) site, we had

little confidence in estimating the liquid water mixing ratio q_l from the radar reflectivity given that the radar beam at its lowest elevation angle of 0.5° was sampling the storm at a significant elevation above ground (e.g., ~ 2.4 km above radar elevation for storms ~ 140 km from the radar). In fact, for many of the events, the radar was sensing hydrometeors aloft that frequently were not reaching the ground. Although the exclusion of q_l in the formal calculation of θ_v results in less accurate values, for 7 of the 10 cases examined, precipitation observed by the mesonet was either absent or very light in the 5-min RFD sampling analysis periods. Thus, only small errors in θ_v calculations are expected for most of the RFD cases analyzed. Significant precipitation was experienced by at least part of the mesonet in three of the events analyzed. For instance, had the radar reflectivity been 45 dBZ in these cases, an overestimate in θ_v of about 0.4 K would be incurred from neglecting q_l based on the parameterization of Rutledge and Hobbs (1984).

CAPE and CIN were calculated using the nearest sounding modified to be representative of the prestorm environment. Rapid Update Cycle model (Benjamin et al. 2004) analysis data were used as guidance for making thermodynamic adjustments where necessary. Surface data within each sounding were represented by averaged mesonet temperature and dewpoint observations for each RFD quadrant (specified later in this section). Surface elevation for the modified soundings was adjusted to be consistent with the elevation of the particular event.

To obtain the perturbation equivalent potential temperature θ'_e and perturbation virtual potential temperature θ'_v , base states were calculated by linearly interpolating 10-min-average inflow observations that were taken by the mesonet. This method was preferred over using the nearest prestorm automated surface observing station (ASOS) or automated weather observing station (AWOS) readings for determining inflow base states for ANSWERS dataset analysis given the mesoscale thermodynamic gradients that usually existed in the region. Thermodynamic calculations of θ_e and θ_v utilizing data from the nearest prestorm ASOS or AWOS station sometimes differed by up to several degrees from the mesonet inflow data.

Ten RFD events (Table 1) that were associated with tornadic and nontornadic RFDs have been selected for thermodynamic analysis and intergroup comparison. To be considered a distinctive RFD event, the RFD must have been associated with a unique hook echo of a supercell thunderstorm (Browning and Donaldson 1963; Fujita 1973; Markowski 2002a). For each RFD event analyzed, a mesocyclone centroid was identified.

TABLE 1. RFD events in chronological order with RFD quadrant sampling percentages. Abbreviations for tornadic events and nontornadic events are TOR and NON, respectively. Dates are given in local time. Time is the radar scan time utilized for analysis in UTC.

Event	Type	Date	Location	Time (UTC)	F rating	Percentage of quadrant sampled			
						I	II	III	IV
1	TOR	9 Jun 2003	Springview, NE	2300	F0	20	40	30	0
2	NON	9 Jun 2003	Newport, NE	2340	—	30	80	70	0
3	TOR	9 Jun 2003	O'Neill, NE	0054	F3	0	0	30	50
4	NON	11 Jun 2003	Vivian, SD	2358	—	0	70	80	20
5	NON	11 Jun 2003	Presho, SD	0034	—	0	0	80	80
6	NON	11 Jun 2003	Kennebec, SD	0056	—	0	0	80	60
7	NON	24 Jun 2003	Cavour, SD	2353	—	0	0	80	0
8	NON	24 Jun 2003	Iroquois, SD	0013	—	0	0	70	30
9	TOR	24 Jun 2003	Manchester, SD	0042	F4	0	0	70	0
10	TOR	24 Jun 2003	Spirit Lake, SD	0127	F1	0	10	80	0

When possible, the positions were found using WSR-88D and Doppler on Wheels (DOW; Wurman et al. 1997) radar velocity data. In cases where the mesocyclone was a large distance from a WSR-88D and poorly resolved, low-level mesocyclone positions were generally estimated by using tornado damage survey position data (documented by the project) with time-referenced videography and by videographic triangulation of wall clouds and tornadoes from multiple viewing angles and positions. In these cases, the wall cloud and tornadoes were assumed to be positioned in the low-level mesocyclone center. In 7 of the 10 cases, the analysis times were chosen to be within 5 min of tornadogenesis or tornadogenesis failure. For the remaining 3 cases, the analysis time was 5–10 min from the time of tornadogenesis or tornadogenesis failure. The time of tornadogenesis failure was defined as the time of strongest rotation determined by either DOW data or by visual reference (necessitated by the sometimes large distance to the nearest WSR-88D).

Data points were plotted relative to WSR-88D or DOW radar data using time-to-space conversion as described by MSR2002. This process put the observational mesonet data into the storm's positional frame of reference. The supercell radar echoes were assumed to be in steady state for 5-min periods that approximate the time for a single WSR-88D volume scan. Although the recorded sampling rate by the mesonet stations was every 2 s, 12-s data averages were used in the analysis to remove very small time-scale fluctuations.

Because of logistical limitations, the area sampled in each RFD varied between events. Therefore, attempts have been made to quantify the density of observations in each event. The RFDs were broken down into four quadrants enclosed in a 4-km radius circle centered on the low-level mesocyclone centroid as shown in Fig. 1 (adopted from MSR2002). The line that separates

quadrants I and IV from II and III passes through the low-level mesocyclone center and is parallel to the neck of the hook echo (Forbes 1978). A 1-km buffer was then placed around each data point for each event to estimate the total percentage (to the nearest 10%) of each quadrant sampled within 1 km by the mesonet. Table 1 presents the percentages of each quadrant sampled for each event as well as the tornadic character of the event. Consistent with project objectives, quadrant III was sampled for all the events with the majority

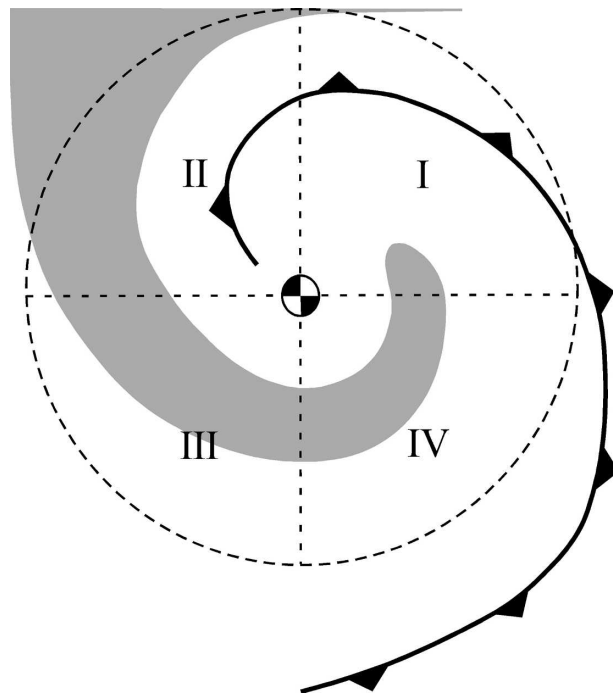


FIG. 1. RFD quadrants, where the gray-shaded region represents supercell idealized radar reflectivity hook signature. Centroid of low-level mesocyclone is indicated along with the RFD boundary. The schematic was adapted from MSR2002.

TABLE 2. The θ'_e and θ'_v sample means by quadrant. NON represents a nontornadic event, TOR represents a tornadic event of F0–F1 intensity, and boldface TOR represents a tornadic event of F2 or greater intensity.

Event	Type	θ'_e (K) quadrant mean				θ'_v (K) quadrant mean			
		I	II	III	IV	I	II	III	IV
1	TOR	-2.0	-2.6	-2.9	—	-1.1	-1.3	-1.3	—
2	NON	-4.6	-4.7	-3.9	—	-5.7	-5.6	-5.1	—
3	TOR	—	—	1.0	0.9	—	—	-0.1	-0.1
4	NON	—	-0.7	-0.3	-1.1	—	0.1	-0.7	-0.6
5	NON	—	—	-4.6	-4.7	—	—	-1.3	-1.3
6	NON	—	—	-3.8	-3.3	—	—	-3.4	-2.5
7	NON	—	—	-1.3	—	—	—	-0.4	—
8	NON	—	—	-13.1	-12.8	—	—	-2.5	-3.1
9	TOR	—	—	-2.7	—	—	—	-0.6	—
10	TOR	—	-1.4	-2.0	—	—	0.4	-0.5	—

of these having excellent quadrant area coverage. Quadrants II and IV were moderately sampled. Because of logistical and safety considerations, quadrant I was rarely sampled. Although the number of events in this study is small compared with MSR2002, the intergroup RFD thermodynamic differences, especially in the more frequently sampled RFD quadrants, are meaningful when utilized in a comparative context with the MSR2002 findings.

3. Results

For each RFD quadrant, mean values for θ'_e and θ'_v (Table 2) were calculated from the mesonet data. The warmest θ_e air (θ'_e of 1.0 K) was found in quadrant III of event 3, which was associated with a tornadic high-precipitation supercell that produced F3 damage. The coldest θ_e air (θ'_e of -13.1 K) was found in quadrant III of event 8, which was associated with a nontornadic RFD. Surprisingly, approximately 30 min after event 8, a violent tornado associated with an RFD having small θ_e and θ_v deficits (Lee et al. 2004) occurred in conjunction with a supercell that resulted from a merger be-

tween the supercell associated with event 8 and a rapidly intensifying cell approaching from the south. The resultant storm rapidly underwent mesocyclogenesis and quickly produced a new hook and RFD. An RFD associated with a weak tornado (event 10) had the warmest θ_v air (θ'_v of 0.4 K) that was present in quadrant II. The coldest θ_v air (θ'_v of -5.7 K) was found in quadrant I of nontornadic event 2. Event 4 yielded noteworthy results as a nontornadic event. It was the second (third) warmest in terms of quadrant-averaged θ'_e (θ'_v), indicating that a comparatively warm RFD is not sufficient for tornadogenesis (also noted by MSR2002).

Values of CAPE and CIN were calculated for all sampled quadrants for each event (Table 3) by inserting the RFD quadrant's mean temperature and dewpoint into the lowest level of each event's modified inflow sounding. All RFDs observed by Project ANSWERS, whether nontornadic or tornadic, contained a substantial amount of CAPE. Nontornadic RFD CAPE values ranged from 1460 to 4232 J kg⁻¹ while tornadic RFD CAPE values ranged from 2542 to 3850 J kg⁻¹. Interestingly, the highest quadrant-averaged CAPE was found within a nontornadic RFD (event 7). The con-

TABLE 3. CAPE and CIN sample means by quadrant. Table designators as in Table 2.

Event	Type	CAPE (J kg ⁻¹) quadrant mean				CIN (J kg ⁻¹) quadrant mean			
		I	II	III	IV	I	II	III	IV
1	TOR	2677	2638	2542	—	122	131	133	—
2	NON	2316	2334	2431	—	273	270	257	—
3	TOR	—	—	3231	3201	—	—	118	117
4	NON	—	2216	2361	2285	—	30	41	34
5	NON	—	—	1499	1534	—	—	105	100
6	NON	—	—	1460	1576	—	—	174	146
7	NON	—	—	4232	—	—	—	14	—
8	NON	—	—	2009	2056	—	—	122	124
9	TOR	—	—	3801	—	—	—	16	—
10	TOR	—	3850	3749	—	—	3	13	—

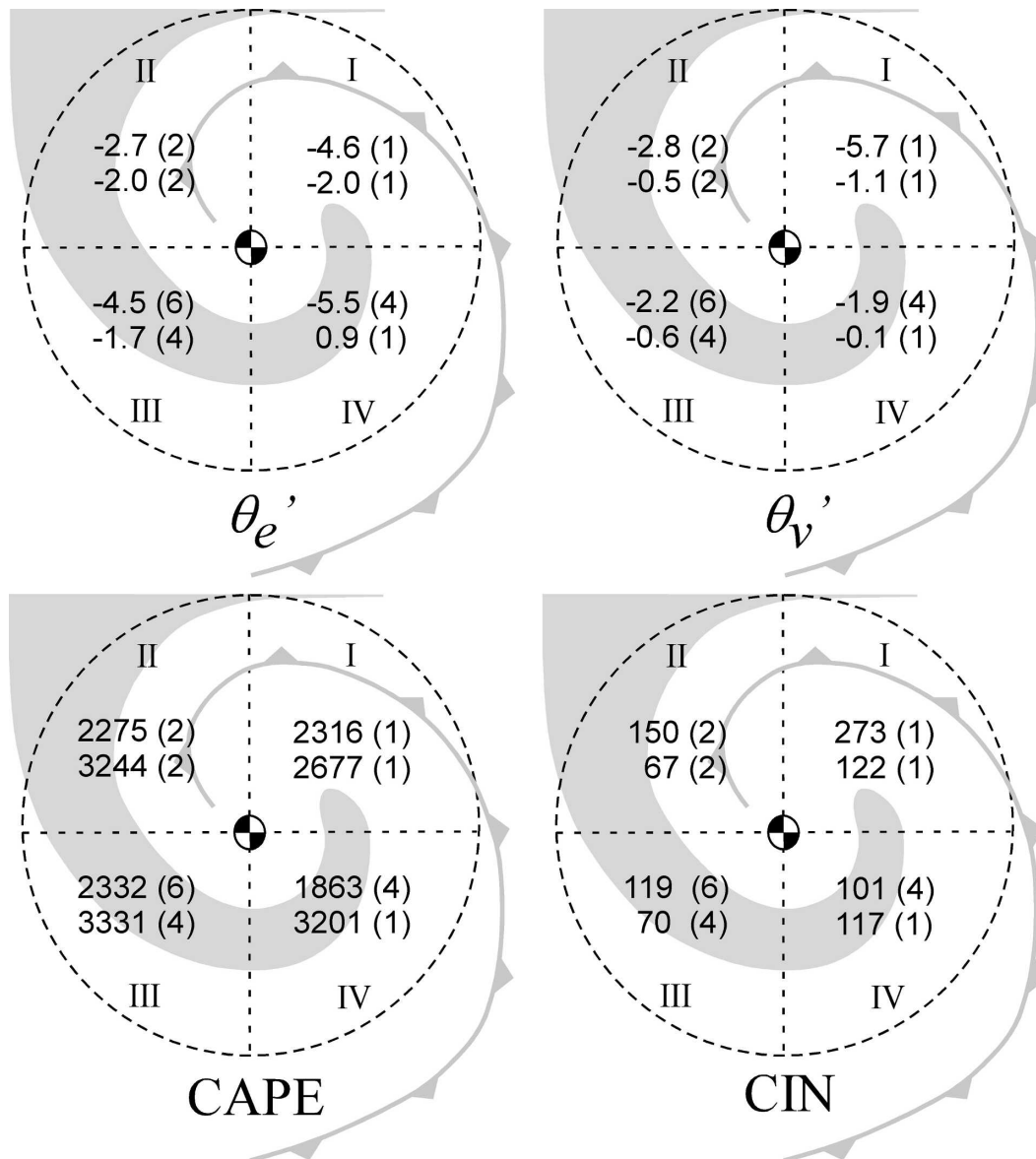


FIG. 2. (top) Nontornadic and (bottom) tornadic RFD group mean quadrant values of θ_e' , θ_v' , CAPE, and CIN. The number of events analyzed for a given quadrant is shown in parentheses.

siderable CAPE values found in the RFDs are broadly reflective of the moderate–high CAPE environments for which these case day supercells formed, even when allowing for sometimes substantial deficits in RFD thermodynamic quantities evident in Table 2. CIN values for both tornadic and nontornadic RFDs ranged from 3 to 273 J kg^{-1} , with the greatest amount of CIN being found for a nontornadic RFD in event 2. One should view the CAPE and CIN magnitude estimates with caution because of the difficulty in establishing a truly representative sounding for the near-storm environment.

Mean RFD quadrant thermodynamic and stability statistics were calculated to compare nontornadic and tornadic event groupings as shown in Fig. 2. Because of logistical limitations and project objectives, certain quadrants were sampled more often than others. Given the smaller number of cases in comparison with MSR2002, the signals from relative group differences are more consequential for well-sampled quadrants such as quadrant III. The tornadic RFD group generally had the smallest θ_e' perturbations (warmest relative θ_e' values). Trends in θ_v' were very similar to θ_e' trends, with the tornadic RFD group having the smallest per-

TABLE 4. Mean RFD θ'_e , θ'_v , CAPE, and CIN (comprising all quadrants) associated with nontornadic and tornadic event groupings.

	θ'_e (K)	θ'_v (K)	CAPE (J kg ⁻¹)	CIN (J kg ⁻¹)
Nontornadic	-4.5	-2.5	2178	130
Tornadic	-1.5	-0.6	3211	82

turbations. Considerably larger CAPE values were associated with the tornadic RFD group. Mean RFD CIN values were generally higher for the nontornadic group.

To condense the characterization of RFD signals present in the dataset, mean thermodynamic and stability parameters were calculated for nontornadic and tornadic event type groupings by applying a frequency-weighted average that comprised all available RFD quadrants (Table 4). RFDs associated with tornadoes had an average θ'_e value 3.0 K warmer than nontornadic RFDs. RFDs associated with tornadoes had an average θ'_v value 1.9 K warmer than nontornadic events. These group differences are similar, albeit somewhat smaller for θ'_v , than those of MSR2002, who found that in terms of mean θ'_e and θ'_v , tornadic RFDs were warmer than nontornadic RFDs by 3–5 K and 3–4 K, respectively. On average the CAPE was 1033 J kg⁻¹ greater in RFDs associated with tornadoes than in RFDs associated with nontornadic supercells. If we assume that 20%–25% of the CAPE was located below 500 mb (as noted by MSR2002) for a representative sample of soundings, then an additional 207–258 J kg⁻¹ of sub-500-mb CAPE was present in tornadic RFDs when contrasted with nontornadic RFDs. These values are roughly comparable to the 300 J kg⁻¹ difference for these groups found by MSR2002. Unlike the large intergroup difference in CIN found by MSR2002 (150–200 J kg⁻¹), a much smaller difference of 48 J kg⁻¹ in mean RFD CIN between nontornadic and tornadic events was present in the ANSWERS dataset.

Recognizing the limitations of the dataset size and noting the relatively large θ'_e values of event 8, we wished to assess the impact that event 8 had on the intergroup θ'_e RFD signal. For reference, although event 8 featured large θ'_e values relative to the other 9 events, these values were not anomalously large when compared with the MSR2002 RFD dataset. To evaluate the influence that event 8 had on the nontornadic group mean RFD θ'_e , this event was removed from the group mean θ'_e calculation. While the nontornadic group mean θ'_e was reduced to -3 K, this value did not change sufficiently to alter the broader signal of the intergroup comparison.

4. Summary and discussion

Data collected during Project ANSWERS afforded an opportunity to test associations established by MSR2002 between RFD thermodynamic characteristics and supercell tornadic activity on a set of events from the northern plains. Although only 10 cases are analyzed in this research, several thermodynamic signals were detected:

- On average, RFDs associated with tornadic supercells had surface θ_e and θ_v values only slightly lower than storm inflow values.
- RFDs associated with nontornadic supercells, on average, displayed θ_e and θ_v values that were colder relative to storm inflow values than their respective tornadic counterparts.
- On average, RFD CAPE in tornadic events was larger than for nontornadic events, while the RFD CIN was smaller for tornadic events than for nontornadic events.

The thermodynamic signals from the ANSWERS RFD dataset analysis are consistent with the guiding hypothesis stated in the introduction; however, in regard to RFD CAPE, even nontornadic cases had significant surface-based CAPE.

The relative coolness of the nontornadic RFDs (exhibited by θ'_e) with respect to RFDs associated with tornadoes suggests that air parcels in nontornadic RFDs may experience a greater vertical displacement or greater degree of midlevel air entrainment. In the case of θ'_v , the coolness of these RFDs is also likely indicative of a larger contribution from evaporative cooling within the hook echo. As noted by one of the reviewers, the relatively small θ'_e values and implied small vertical displacements for RFD parcels arriving at the surface in tornadic supercells appear in contradiction to the classic airflow schematic for supercells presented by Lemon and Doswell (1979). In this airflow schematic, the RFD begins in the upper midtroposphere with parcels mixing with air at lower levels as they descend. Presumably, depending upon the extent of mixing in the descent, the parcels would retain some θ_e signature from the midlevel source regions, which generally does not appear to be the case for tornadic supercells. Another possible explanation for the small RFD θ'_e values includes a scenario where parcel vertical displacements are considerable but the RFD source region contains updraft air (with the approximate θ_e values of the storm inflow) that is forced to descend by a downward-directed dynamic pressure gradient force (or by precipitation loading). In either case, the recent RFD observations raise questions about the applicabil-

ity of the classic RFD airflow conceptual model to tornadic supercells and may be indicative of dynamically different modes in which RFD parcels arrive at the surface in tornadic and nontornadic supercells. The reader is referred to Markowski et al. (2002) for a more detailed discussion of RFD forcing mechanisms. Much research is needed concerning the origin regions and forcing mechanisms for the RFD. While a thermodynamically "mild/warm" RFD appears to be essential for tornadogenesis, as events 4 and 7 demonstrated, a thermodynamically warm RFD is not sufficient for tornadogenesis.

Even with a considerably smaller number of cases, results from the ANSWERS RFD analysis are generally similar to those found by MSR2002, with specific regard to RFD thermodynamic characterization associated with supercell tornadic activity. The consistency of the findings between the RFD thermodynamic analyses for the northern plains ANSWERS cases and those of MSR2002 is indicative of a robust thermodynamic signal differentiating RFDs associated with tornadic events from those linked with nontornadic events.

While the associations developed in this research are limited to those from thermodynamic analysis, an assimilation of complimentary kinematic data in the analysis would provide more latitude in building physical relationships. We anticipate that future field programs such as the next phase of the Verification of the Origins of Rotation in Tornadoes Experiment (Rasmussen et al. 1994) will provide an array of comprehensive kinematic and thermodynamic datasets with which to build these physical relationships.

Acknowledgments. This study was funded by NSF Grants ATM-0102579 and ATM-0432408. The authors thank all Project ANSWERS participants for their considerable contributions. The Department of Atmospheric Sciences at Texas Tech University provided a mesonet station and support for the first author's participation in Project ANSWERS. A significant portion of the analysis presented is a distillation of the first author's master's thesis research. The first author appreciatively acknowledges the support from his advisor, Prof. John Schroeder, at Texas Tech University. Dr. Josh Wurman (Center for Severe Weather Research) graciously contributed DOW data, which Dr. David Dowell (Cooperative Institute for Mesoscale Meteorological Studies) processed and provided. The authors recognize Patrick Skinner for his substantial contributions in developing quality control programs and in

postprocessing the mesonet data. Erik Crosman and Brian Guarente are acknowledged for their efforts in managing software development and operational aspects of the project. Dr. Matt Gilmore graciously provided assistance for matching the mesonet vehicle tracks with the appropriate elevation for data postprocessing.

REFERENCES

- Benjamin, S. G., and Coauthors, 2004: An hourly assimilation-forecast cycle: The RUC. *Mon. Wea. Rev.*, **132**, 495–518.
- Bolton, D., 1980: The computation of equivalent potential temperature. *Mon. Wea. Rev.*, **108**, 1046–1053.
- Browning, K. A., and R. J. Donaldson, 1963: Airflow and structure of a tornadic storm. *J. Atmos. Sci.*, **20**, 533–545.
- Forbes, G. S., 1978: Three scales of motions associated with tornadoes. U.S. Nuclear Regulatory Commission Contract Rep. NUREG/CR-0363, 359 pp.
- Fujita, T. T., 1973: Proposed mechanism of tornado formation from rotating thunderstorms. Preprints, *Eighth Conf. on Severe Local Storms*, Denver, CO, Amer. Meteor. Soc., 191–196.
- Glickman, T., Ed., 2000: *Glossary of Meteorology*. 2d ed. Amer. Meteor. Soc., 855 pp.
- Lee, B. D., C. A. Finley, and P. Skinner, 2004: Thermodynamic and kinematic analysis of multiple RFD surges for the 24 June 2003 Manchester, South Dakota cyclic tornadic supercell during Project ANSWERS 2003. Preprints, *22d Conf. on Severe Local Storms*, Hyannis, MA, Amer. Meteor. Soc., CD-ROM, P11.2.
- Lemon, L. R., and C. A. Doswell III, 1979: Severe thunderstorm evolution and mesocyclone structure as related to tornadogenesis. *Mon. Wea. Rev.*, **107**, 1184–1197.
- Markowski, P. M., 2002a: Hook echoes and rear flank downdrafts: A review. *Mon. Wea. Rev.*, **130**, 852–876.
- , 2002b: Mobile mesonet observations on 3 May 1999. *Wea. Forecasting*, **17**, 430–444.
- , J. M. Straka, and E. N. Rasmussen, 2002: Direct surface thermodynamic observations within the rear-flank downdrafts of nontornadic and tornadic supercells. *Mon. Wea. Rev.*, **130**, 1692–1721.
- Rasmussen, E. N., J. M. Straka, R. Davies-Jones, C. A. Doswell III, F. H. Carr, M. D. Eilts, and D. R. MacGorman, 1994: Verification of the Origins of Rotation in Tornadoes Experiment: VORTEX. *Bull. Amer. Meteor. Soc.*, **75**, 955–1006.
- Rutledge, S. A., and P. V. Hobbs, 1984: The mesoscale and microscale structure and organization of clouds and precipitation in midlatitude cyclones. XII: A diagnostic modeling study of precipitation development in narrow cold-frontal rainbands. *J. Atmos. Sci.*, **41**, 2949–2972.
- Straka, J. M., E. N. Rasmussen, and S. E. Fredrickson, 1996: A mobile mesonet for finescale meteorological observations. *J. Atmos. Oceanic Technol.*, **13**, 921–936.
- Wurman, J., J. M. Straka, E. N. Rasmussen, M. Randall, and A. Zahrai, 1997: Design and deployment of a portable, pencil-beam, pulsed, 3-cm Doppler radar. *J. Atmos. Oceanic Technol.*, **14**, 1502–1512.